

# Supporting Information

## **Therapeutic Nanoplatfoms with Bacteria-Specific Activation for Directional Transport of Antibiotics**

Yunjian Yu, Tianqi Zhang, Xijuan Dai, Xiaomei Dai, Xiaosong Wei, Xinge Zhang\*  
and Chaoxing Li

Key Laboratory of Functional Polymer Materials of Ministry of Education, Institute  
of Polymer Chemistry, College of Chemistry, Nankai University, Tianjin 300071,  
China

Corresponding author: E-mail address: [zhangxing@nankai.edu.cn](mailto:zhangxing@nankai.edu.cn)

## Materials and Methods

### 1. Materials

Acryloyl chloride was prepared by refluxing acrylic acid and thionyl chloride at 75 °C for 8 h and freshly distilled before used. D-Glucosamine hydrochloride was supplied by Beijing Ouhe Technology Co. Ltd. (Beijing, China). 3-Aminophenylboronic acid monohydrate was purchased from Nanjing Kangmanlin Chemical Industry Co. Ltd. (Nanjing, China). 2,2'-Azobis-(isobutyronitrile) (AIBN) was recrystallized twice from ethanol and dried in vacuum before used. Boron-dipyrromethene (BODIPY) dye-conjugated chain transfer agent was synthesized as reported previously.<sup>1</sup> Acridine orange (AO, Fluk) and ethidium (EB, Fluk) were bought from Beijing Solarbio Science & Technology Co. Ltd. (Beijing, China). 3-(4,5-Dimethylthiazol-2-yl)-2,5-diphenyltetrazolium bromide (MTT) was obtained from Beyotime Institute of Biotechnology (Nantong, China). Dulbecco's modified Eagle's medium (DMEM), minimum essential medium (MEM), penicillin/streptomycin solution, trypsin, nonessential amino acid, and fetalbovine serum (FBS) were purchased from Gibco (CA, America). The mouse embryonic fibroblast cell line, NIH3T3, was obtained from American Type Culture Collection. Triclosan was bought from Sahn Chemical Technology Co. Ltd. (Shanghai, China). Other reagents were of analytical grade and used as received. *Staphylococcus aureus* (*S.aureus*) ATCC 6538, *Bacillus amyloliquefaciens* (*B. amyloliquefaciens*) ATCC 23842, *Escherichia coli* (*E. coli*) ATCC 8739 and *Pseudomonas aeruginosa* (*P. aeruginosa*) ATCC 9027 strains were provided by Department of Microbiology of Nankai University (Tianjin, China).

### 2. Synthesis of 3-Acrylamidophenylboronic Acid (AAPBA)

3-acrylamidophenylboronic acid (AAPBA) was prepared using the modified method described by Lee et al.<sup>2</sup> Briefly, 3-aminophenylboronic acid monohydrate (1.0 g, 6.44 × 10<sup>-3</sup> mol) was dissolved in sodium hydroxide solution (8 mL, 0.0258 mol) and

cooled in an ice bath. Acryloyl chloride (0.64 mL,  $8 \times 10^{-3}$  mol) was added dropwise to 3-aminophenylboronic acid monohydrate solution over 1 h. The reaction mixture was stirred for further 2 h at room temperature and adjusted to pH 8 using 0.1 M HCl. The resulting precipitation was filtered and washed with cold water. The precipitate was dissolved in distilled water after heating to 80 °C, and the insoluble residues were refiltered, and dried under a vacuum.

### **3. Synthesis of Poly(2-(Acrylamido) Glucopyranose) (pAGA)**

2-Acrylamido glucopyranose (AGA) was synthesized by the previously reported method.<sup>3</sup> Typically, D-glucosamine hydrochloride (6.0 g,  $2.78 \times 10^{-2}$  mol) and potassium carbonate (6.41 g,  $2.78 \times 10^{-2}$  mol) were dissolved in methanol (150 mL) in a 250 mL single neck round-bottom flask. The flask was cooled to -10 °C using an acetone/ice bath before acryloyl chloride (2.034 mL,  $2.50 \times 10^{-2}$  mol) was added dropwise into the mixture under vigorous stirring. The mixture was stirred in ice bath for 30 min and then reacted for another 3 h at room temperature. The crude mixture was concentrated under reduced pressure to off-white slurry. The slurry was purified via silica gel column chromatography using dichloromethane/methanol (v/v, 4:1) as eluent. The white solid exited the column with the R<sub>f</sub> value of 0.33, with 58% conversion obtained gravimetrically.

pAGA was prepared via reversible addition fragmentation transfer (RAFT) polymerization using BODIPY-RAFT as RAFT agent, AIBN as initiator by the previously reported method. Briefly, AGA and a certain amount of BODIPY-RAFT and AIBN were added into a mixed solvent DMF/H<sub>2</sub>O (v/v, 9:1), the feed molar ratio of [AGA]:[BODIPY-RAFT]:[AIBN] = 60:1:0.2. After the resultant mixture was degassed by bubbling nitrogen for 30 min, the reaction was conducted at 70 °C for 12 h and was quenched in an ice bath for 10 min. The resultant products were isolated by

precipitating with acetic ether three times, and drying under vacuum, which was named as pAGA<sub>60</sub>.

#### 4. Synthesis of Random and Block Phenylboronic Acid-Based Glycopolymers

Random copolymer p(AAPBA-*r*-AGA) was synthesized by RAFT polymerization using AAPBA and AGA as monomers, BODIPY-RAFT as RAFT agent, AIBN as initiator, and DMF/water (v/v, 19:1) as a mixed solvent. The copolymerization was performed at [AAPBA]:[AGA]:[CTA]:[AIBN]= 45:15:1:0.2. After the solution was purged with N<sub>2</sub> for 30 min, the reaction system was allowed to stir at 70 °C for 12 h, and then polymerization was quenched by cooling in an ice bath for 10 min. The resultant copolymer was precipitated, filtered, washed with acetic ether and subsequently dried under a vacuum. By changing the feed molar ratio of AAPBA and AGA to BODIPY-RAFT, we obtained three distinct random copolymers named as p(AAPBA<sub>45</sub>-*r*-AGA<sub>15</sub>), p(AAPBA<sub>30</sub>-*r*-AGA<sub>30</sub>), and p(AAPBA<sub>15</sub>-*r*-AGA<sub>45</sub>), respectively.

pAAPBA was synthesized by RAFT polymerization, using BODIPY-RAFT as RAFT agent, AIBN as initiator, dimethylformamide (DMF) as solvent. The copolymerization was performed at [AAPBA]:[BODIPY-RAFT]:[AIBN] = 60:1:0.2 then the mixture was purged with nitrogen for 30 min and transferred to a water bath preheated to 70 °C. The reaction was quenched after 12 h by cooling in an ice bath for 10 min. The resultant polymer was isolated by precipitating with acetic ether three times, and drying under vacuum. By changing feed molar ratio of AAPBA to BODIPY-RAFT (60:1, 45:1, 30:1 and 15:1), three different homopolymers were obtained, marked as pAAPBA<sub>60</sub>, pAAPBA<sub>45</sub>, pAAPBA<sub>30</sub>, and pAAPBA<sub>15</sub> respectively.

RAFT copolymerization was performed at [AGA]/[BODIPY-RAFT]/[AIBN] =

45:1:0.2 using AGA as monomer, homopolymer pAAPBA as macroRAFT agent, AIBN as initiator, and DMF/water (v/v, 19:1) as mixed solvents. The reaction system was placed in a preheated water bath at 70 °C for 12 h following nitrogen purging for 30 min. The polymerization was quenched by cooling in an ice bath for 10 min. The resultant polymer was obtained by precipitating with acetic ether for three times, and drying under vacuum. By changing the ratio of macroRAFT (pAAPBA) to the AGA, we obtained three distinct block copolymers and these were named as p(AAPBA<sub>15</sub>-*b*-AGA<sub>45</sub>), p(AAPBA<sub>30</sub>-*b*-AGA<sub>30</sub>) and p(AAPBA<sub>45</sub>-*b*-AGA<sub>15</sub>).

## 5. Characterization of Glycopolymers

Proton nuclear magnetic resonance (<sup>1</sup>H NMR) spectra were recorded at room temperature using a Varian Unity-plus 400 NMR spectrometer. FT-IR spectra were recorded on a Fourier Transform Infrared Spectrometer (FTS-6000, Bio-Rad Co.) using a KBr tablet containing the sample powder at a resolution of 8 cm<sup>-1</sup>. The thermogravimetric analysis of copolymer, using 10 mg per sample, was conducted in nitrogen using a thermogravimetric analyzer (TGA, STA409PC) at a heating rate of 10 °C/min.

## 6. Preparation of Copolymeric Nanoparticles

Copolymeric nanoparticles were prepared according to the previously reported method.<sup>4,5</sup> In brief, 10 mg of amphiphilic glycopolymer was dissolved in 1 mL of a mixed solvent containing DMSO and water (v/v, 4:1), and then 7 mL of water was slowly added to the solution under vigorous stirring. The procedure yielded an opalescent suspension and the solution was incubated overnight at room temperature with continuous stirring. After 12 h, the solution was transferred to a dialysis tube (MWCO 3500) and dialyzed against water with rapid stirring for 24 h. The organic solvent was removed by changing water every 3 h, and then the nanoparticle solution

was centrifuged at 12000 rpm for 30 min. Finally, blank nanoparticles were obtained after freeze-drying.

Triclosan-loaded nanoparticles were prepared in a similar method. 3 mg of Triclosan and 10 mg of polymer were dissolved in 1 mL of a mixed solvent of DMSO and H<sub>2</sub>O (4:1, v/v) and then 7 mL of water was slowly added to the solution under vigorous stirring. The resulting Triclosan-glycopolymer solution was then prepared as described for the empty nanoparticles. Finally, the precipitate was washed with deionized water and centrifuged three times prior to lyophilization. The weight of obtained Triclosan-loaded nanoparticles was recorded by analytical balance and the amount of the encapsulated Triclosan was calculated by the corresponding mass of polymer. Encapsulation efficiency (EE) and loading capacity (LC) of Triclosan were calculated using the equation (2.1) and (2.2):

$$EE = \frac{\text{Weight of Triclosan in NPs}}{\text{Weight of NPs}} \times 100\% \dots\dots\dots(2.1)$$

$$LC = \frac{\text{Weight of Triclosan in NPs}}{\text{Weight of Triclosan used for encapsulation}} \times 100\% \dots\dots\dots(2.2)$$

## 7. Characterization of Nanoparticles

Hydrodynamic diameter ( $D_H$ ), size distribution (PDI) and Zeta potential of nanoparticles were characterized by dynamic light scattering (DLS) using a Malvern Zetasizer Nano S apparatus equipped with a 4.0 mV laser operating at  $\lambda = 636$  nm. All measurements were performed in triplicate at a scattering angle of 90°. The morphological characteristics of nanoparticles were observed using transmission electron microscope (TEM, Philips EM400ST). Samples were placed on copper grids coated with Formvar films for observation under TEM.

## 8. Hemolytic Assay

The hemolysis assay was performed using human blood. Briefly, human blood was centrifuged at 1000 rpm for 3 min using centrifuge (Cence, H1850) and serum was discarded. The red blood cells were washed three times using phosphate buffer solution (PBS, 0.01 M, pH 7.4) and diluted using PBS with the volume fraction of 1%. We used triton-100 as positive control (+) and PBS as negative control (-). Red blood cells (0.75 mL) were added into various concentrations of nanoparticles (0.75 mL). After gently shaking, the samples were co-cultured at 37 °C for 45 min. After centrifugation, the supernatant was recorded the absorbance value at 576 nm using UV-vis spectrometer (Shimadzu, UV-2550). The percentage of hemolysis (Hemolysis %) was calculated from the equation (2.3), where Abs, Abs(-) and Abs(+) are the absorbance of blending samples, the negative control of PBS, and the positive control of triton-100, respectively.

$$\text{Hemolysis\%} = \frac{\text{Abs} - \text{Abs}_{(-)}}{\text{Abs}_{(+)} - \text{Abs}_{(-)}} \times 100\% \dots\dots\dots(2.3)$$

## 9. Cell Viability

Cell viability of block and random copolymers was evaluated by using NIH3T3 cells. The cell lines were cultured in Dulbecco's modified Eagle's medium (DMEM, Gibco) supplemented with 10% fetal bovine serum, 1% penicillin/streptomycin and 1% nonessential amino acid in 5% CO<sub>2</sub>/95% air at 37 °C. Cells were seeded in a 96-well plate at a density of 10<sup>4</sup> cells per well. The copolymeric nanoparticles were diluted with culture medium to achieve the predetermined concentrations. The media in the wells were replaced with the pre-prepared sample solution. After 24 h of incubation, 10 µL of MTT solution was added into each well and the mixtures were incubated for further 4 h. The medium was removed and 150 µL of DMSO was added to each well to dissolve the formazane crystals. The optical density was read on a microplate

reader at 492 nm in triplicate. Relative cell viability was calculated as a percentage compared with that of untreated control.

#### **10. Bacterial Adhesion of Phenylboronic Acid-Based Glycopolymers**

The adhesion effects of copolymeric nanoparticles with different compositions to different types of bacteria were evaluated by co-culture, and the bacteria assemblages were observed by confocal laser scanning microscopy (CLSM, Leica, TCS SP8). Firstly, Bacteria were cultured overnight at 37 °C in LB medium and then 1 mL bacterial suspension was concentrated at 4000 rpm for 5 min, washed with PBS for three times and redispersed in 1 mL PBS (pH 7.4). A solution of nanoparticles at a concentration of 1.0 mg/mL was prepared with PBS buffer at pH 7.4 and 1 mL was withdrawn and co-cultured with the above prepared bacterial suspension at 37 °C under static conditions for 2 h. Then the mixtures were concentrated and washed with PBS for several times to remove nanoparticles that do not adhere to bacteria. The samples were dispersed in a small amount of glycerol, mixed evenly prior to dropping 10 µL on the slide and covered with coverslips. The fluorescence photographs of bacteria clusters were obtained by CLSM, the maximum excitation and emission wavelength of BODIPY were 503 and 513 nm, respectively.

The above procedures were repeated after replacing PBS from pH 7.4 to pH 6.5 .

#### **11. In Vitro Bacteria-Responsive Drug Release**

In vitro Triclosan release from different nanoparticles at pH 6.5 and pH 7.4 was investigated as the following method. The Triclosan-loaded copolymeric nanoparticles were formulated by PBS buffer (pH 7.4) at a concentration of 1 mg/mL, of which the final volume was 9 mL. Then dispensed the prepared nanoparticles into two dialysis bags, one of which was further added a bacterial suspension (0.5 mL, OD<sub>600</sub> = 2.0) prepared with PBS buffer at pH 7.4 and set as experiment group, another



was added an equal volume of PBS (pH 7.4) and set as control group. The two dialysis bags were placed in a centrifuge tube containing 20 mL of PBS buffer (pH 7.4) respectively and were incubated at  $37 \pm 0.5$  °C with shaking (100 rev/min). At a predetermined time, 1 mL of sample in the centrifuge tube outside the dialysis bag was withdrawn and replaced with the same volume of fresh medium. The concentration of the released drug was calculated from the standard curve of Triclosan. Each sample was analyzed in triplicate and results were reported as mean  $\pm$  standard deviation ( $n=3$ ).

The above procedures were repeated after replacing PBS buffer at pH 7.4 into PBS at pH 6.5.

## **12. Bacterial Growth Inhibitory Assay**

Bacteria were cultured overnight at 37 °C in Luria-Bertani (LB) medium and then diluted with LB medium to be an absorbance of 0.4 at 600 nm ( $OD_{600} = 0.4$ ) measured by UV-vis spectrometer. 0.5 mL of bacterial suspension was mixed with an equal volume of 2-fold diluted empty and Triclosan-loaded nanoparticle solutions, and incubated for 8 h at 37 °C. The growth inhibition of bacteria was evaluated by measuring  $OD_{600}$ . Bacterial suspensions treated with an equal volume of PBS were set as the positive control group. Samples incubated with antibacterial materials and broth only were used as the negative control. Substituting the drug-loaded nanoparticle solutions with Triclosan solutions with a same drug concentration and repeated the same operations. Each assay was performed in triplicate.

## **13. The Zone of Inhibition Test**

50  $\mu$ L of the bacterial suspension ( $OD_{600} = 0.5$ ) was inoculated evenly on an LB agar plate. Then, the sample disks containing antimicrobial materials were gently placed at the center of the LB agar plate. After incubation for 10 h at 37 °C, areas of clear

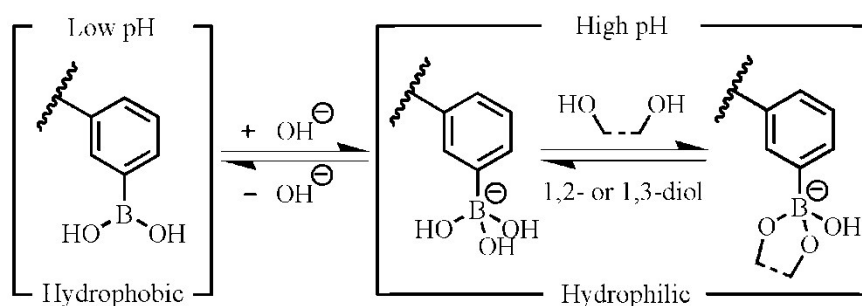
media surrounding the disks indicate that the antimicrobial materials inhibited bacterial growth. The antibacterial activity was evaluated by measuring the diameter of the zone of inhibition around the disks. Sample disks containing PBS was set as the control group.

#### **14. LIVE / DEAD Bacterial Fluorescence Experiments**

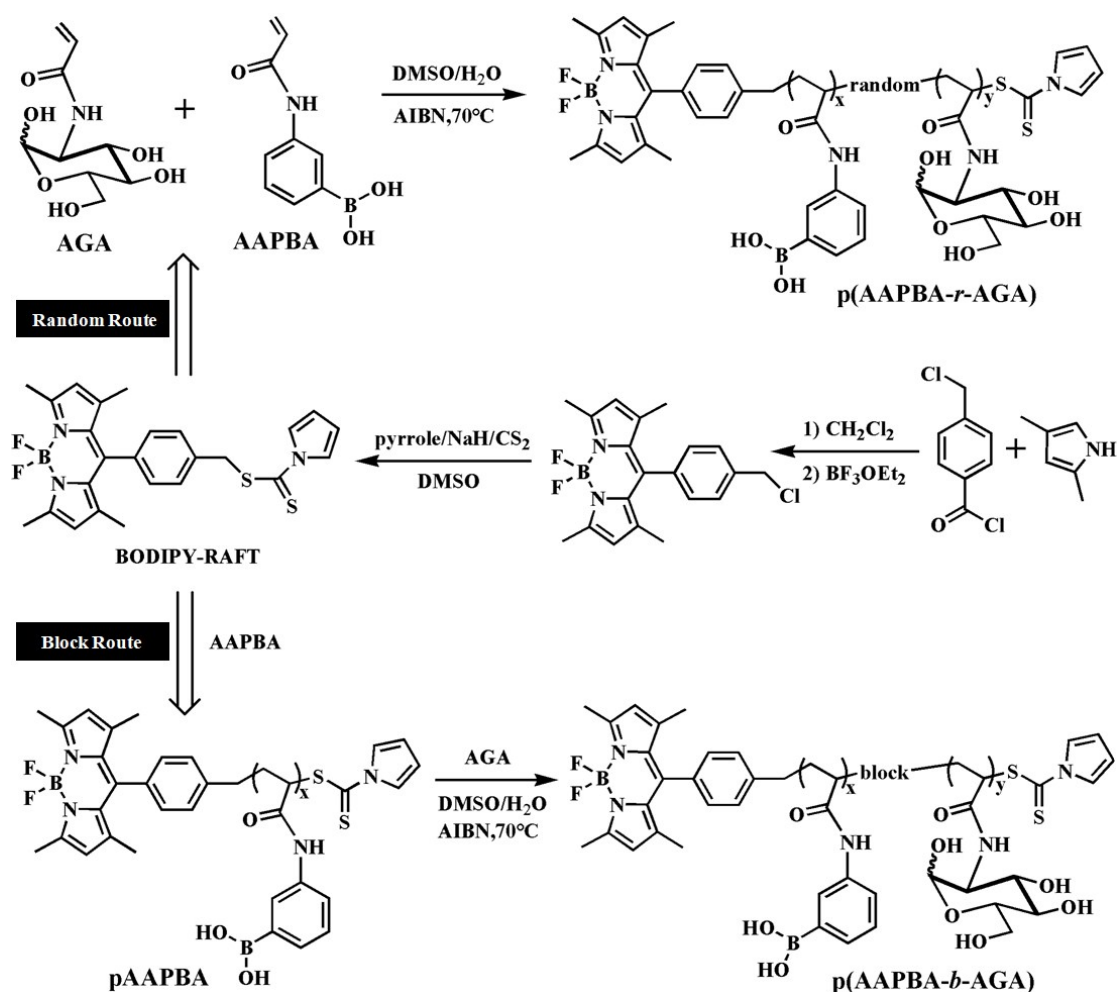
Bacterial suspension (1 mL, OD<sub>600</sub> = 1.0) was centrifuged for 5 min at 4000 rpm and washed three times with PBS. The bacteria were suspended in PBS, and treated for 2 h with copolymeric nanoparticles (1mL, 1.0 mg/mL). Then, the treated bacteria were stained with EB (10 µL, 0.1 mg/mL) at 4 °C for 15 min in darkness. After staining, bacteria were rinsed several times with PBS and observed and imaged using CLSM. Bacteria treated with PBS were set as the control groups. Specially, the control groups were stained with EB (10 µL, 0.1 mg/mL) and AO (10 µL, 0.1 mg/mL) at 4 °C for 15 min in darkness.

#### **15. Preparation of Bacterial Samples for SEM**

Glass slides were treated with saturated NaOH/ethanol solution and then rinsed thoroughly with water. The bacteria treated with materials were tiled on the glass slides, fixed overnight with 2.5% glutaraldehyde and washed with water for three times. Then, bacterial samples were dehydrated using a series of ethanol solutions (30%, 50%, 70%, 90%, 95% and 100% v/v in water) and lyophilized. Bacteria treated with PBS were set as the control groups. The samples were placed on double-sided adhesive conductive carbon tape (3 M), then mounted onto an aluminum stud, coated with platinum and observed using a field-emission scanning electron microscope (SEM, JSM-7500F, Japan).



**Scheme S1.** The equilibrium schematic of boric acid derivatives in the system.



**Scheme S2.** Synthesis of BODIPY-based (A) random copolymer p(AAPBA-*r*-AGA) and (B) block copolymer p(AAPBA-*b*-AGA).

### Synthesis and Characterization of Block and Random Copolymers

Fabrications of block copolymer p(AAPBA-*b*-AGA), random copolymer p(AAPBA-*r*-AGA) and homopolymer pAGA, pAAPBA were carried out by RAFT

polymerization as shown in [Scheme S1](#). A series of copolymers were obtained by changing the molar ratio of monomers to the corresponding BIDIPY as a RAFT agent. To confirm the structure difference,  $^1\text{H}$  NMR spectra of AAPBA, pAAPBA and p(AAPBA-*b*-AGA) were analyzed. In the spectrum of AAPBA, peaks at 5.7, 6.3, and 6.5 ppm were assigned to protons on double bond while signals at 7.0–7.9 ppm were assigned to protons on benzene ring. In comparison with the spectrum of AAPBA, signals of double bond in pAAPBA completely disappeared, and peaks of phenyl group at 6.8–7.8 ppm were retained, confirming the successful preparation of pAAPBA. After copolymerization of pAAPBA and AGA, the new resonance signals in p(AAPBA-*b*-AGA) appeared in the ranges of 0.8–2.2 and 3.0–3.8 ppm, which were assigned to protons from main chain and sugar residue, respectively, indicating p(AAPBA-*b*-AGA) copolymer was synthesized successfully.  $^1\text{H}$  NMR spectra of AAPBA, AGA and p(AAPBA-*r*-AGA) were further analyzed. As shown in Figure 1, signals at 3.2–4.0 ppm were ascribed to protons on the sugar residue in AGA, and peaks at 5.2, 5.8, and 6.3 ppm assigned to protons on double bond. Compared with the spectra of AGA and AAPBA, it is obvious that signals of double bond disappeared and protons on the newly formed main chain generated signals at 0.8–2.4 ppm in the spectrum of p(AAPBA-*r*-AGA). Both typical signals of phenyl (6.8–8.0 ppm) and sugar residue (2.8–3.8 ppm) were preserved in the spectrum of random copolymer. These results imply that block and random copolymers were successfully prepared. The composition ratio of AAPBA and AGA in the copolymer was calculated using  $^1\text{H}$  NMR integral intensity of signals between the 4H in phenyl moieties and 5H in sugar units and the results are shown in [Table S1](#). The integral calculation results are consistent with the feed ratio, and the corresponding block copolymer has a similar composition ratio with the random copolymer.

Compared with the spectra of p(AAPBA-*r*-AGA) and p(AAPBA-*b*-AGA) in Fig. S1A, we found that the features of peaks from sugar residues and phenyl groups in block and random copolymers were different. The results were attributed to the different distribution of sugar and phenylboronic acid moiety in the copolymers.

The structures of the copolymers were further analyzed by infrared spectroscopy. Fig. S1B showed FT-IR spectrums of pAAPBA, p(AAPBA-*b*-AGA) and p(AAPBA-*r*-AGA). In the spectrum of pAAPBA, peak absorption band of 3313  $\text{cm}^{-1}$  was due to N-H stretching. Amide I band was assigned to C=O stretching resulted in an absorption band of 1659  $\text{cm}^{-1}$ , while an absorption band at 1547  $\text{cm}^{-1}$  was attributed to N-H bending vibration (amide II band) of a secondary amide. In addition, the typical absorption bands of phenyl ring in pAAPBA from 1500 to 1350  $\text{cm}^{-1}$  region and absorption peaks at 797 and 711  $\text{cm}^{-1}$  were observed. In comparison with pAAPBA, p(AAPBA-*b*-AGA) maintained the typical absorption of pAAPBA described above. And band in 1200–1000  $\text{cm}^{-1}$  region resulted from C–O stretching corresponding to alkoxyl bond in carbohydrate moiety. The FT-IR spectrum of p(AAPBA-*r*-AGA) was similar to that of p(AAPBA-*b*-AGA), indicating that block and random copolymers were successfully synthesized.

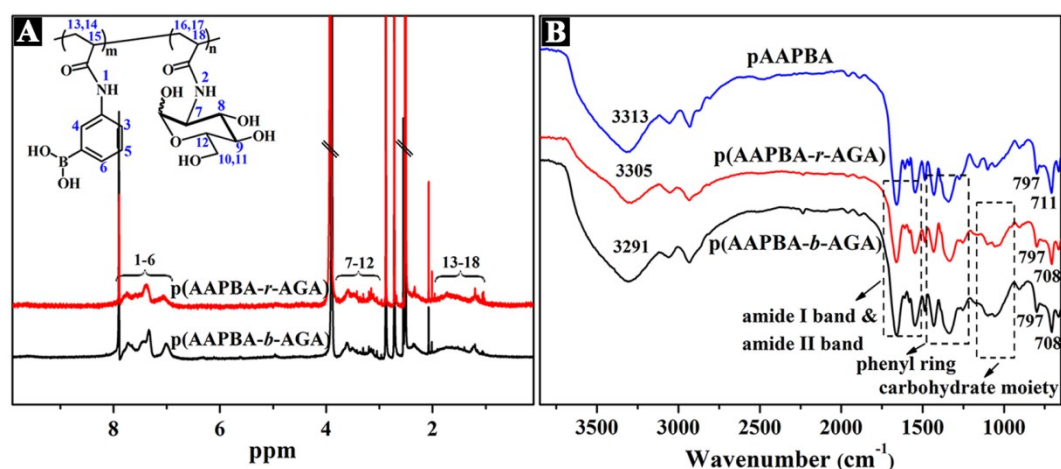


**Fig. S1** (A)  $^1\text{H}$  NMR spectra of p(AAPBA-*r*-AGA) and p(AAPBA-*b*-AGA) (the mixed solvents of DMSO- $\text{d}_6/\text{D}_2\text{O}$ , v/v = 19:1); (B) FT-IR spectra of pAAPBA, p(AAPBA-*r*-AGA), and p(AAPBA-*b*-AGA).

We further performed thermogravimetric analysis to evaluate the effect of copolymer structure on their thermostability. Thermogravimetric (TG) and derivative thermogravimetric (DTG) curves for p(AAPBA<sub>45</sub>-*r*-AGA<sub>15</sub>) and p(AAPBA<sub>45</sub>-*b*-AGA<sub>15</sub>) were shown in Fig. S2. Compared with TG and DTG curves of two copolymers, there was profoundly different degradation phenomenon. It can be seen from DTG curves that there were three distinct degradations at about 57, 200, and 375 °C for p(AAPBA<sub>45</sub>-*r*-AGA<sub>15</sub>), and 62, 161, and 363 °C for p(AAPBA<sub>45</sub>-*b*-AGA<sub>15</sub>), respectively. For two copolymers, the first degradation at 57 °C and 62 °C was assigned to free water and to water linked by hydrogen bonds. The second degradation, which was maximized around 161 °C for p(AAPBA<sub>45</sub>-*b*-AGA<sub>15</sub>) while for p(AAPBA<sub>45</sub>-*r*-AGA<sub>15</sub>) it took place at 200°C, corresponded to the thermal decomposition of the pendent sugar residues. We deduce that the higher temperature in the second degradation for random copolymer was attributed to more boronate complex between phenylboronic acid and sugars with the consequent improvement in thermal stability of pendent sugar residues. The last stage of thermal degradation was assigned to the thermal degradation of the backbone. At this stage, the 30% of weight loss temperature for p(AAPBA<sub>45</sub>-*b*-AGA<sub>15</sub>) was 363 °C, whereas that of p(AAPBA<sub>45</sub>-*r*-AGA<sub>15</sub>) was 375 °C with 43% of weight loss. These results were in accordance with the previous reports. The above results show that the copolymer structure plays an important role in their thermal decomposition.

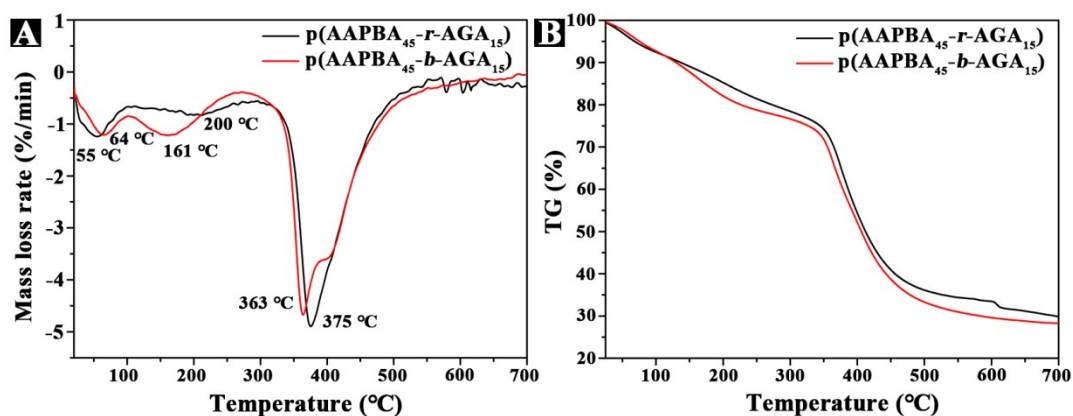


**Fig. S2** Thermal analysis of copolymers: (A) TG and (B) DTG curves for p(AAPBA<sub>45</sub>-r-AGA<sub>15</sub>) (black) and p(AAPBA<sub>45</sub>-b-AGA<sub>15</sub>) (red).

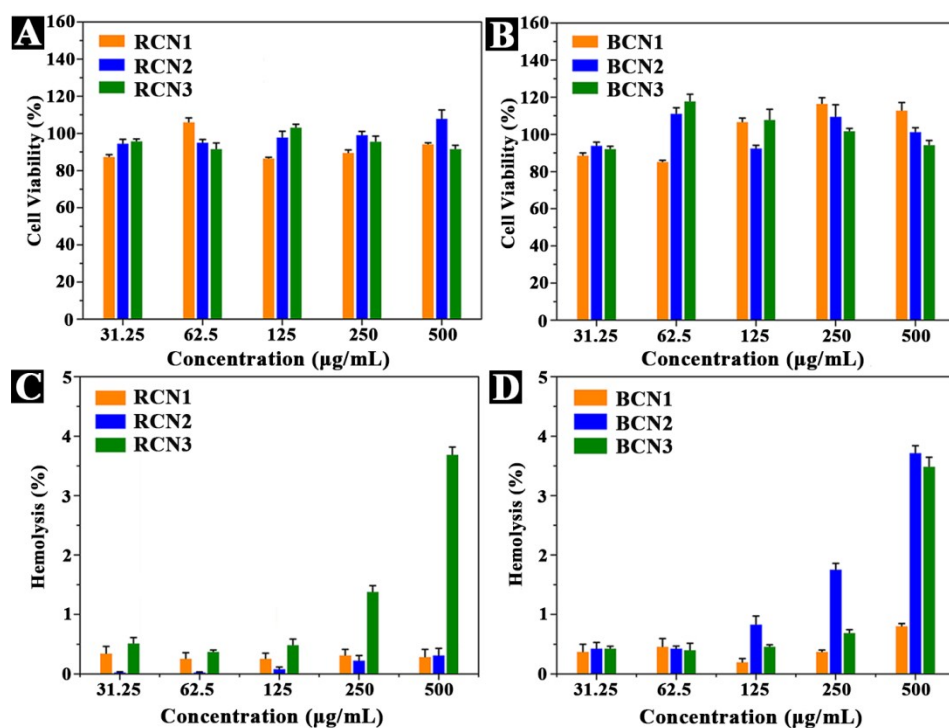


**Fig. S3** Cell viability of NIH3T3 cells after incubation with different concentrations of (A) RCN and (B) BCN for 48 h at 37 °C by MTT assay. Hemolysis of different concentrations of (C) RCN and (D) BCN. Each value represented the mean  $\pm$  SD (n = 5).



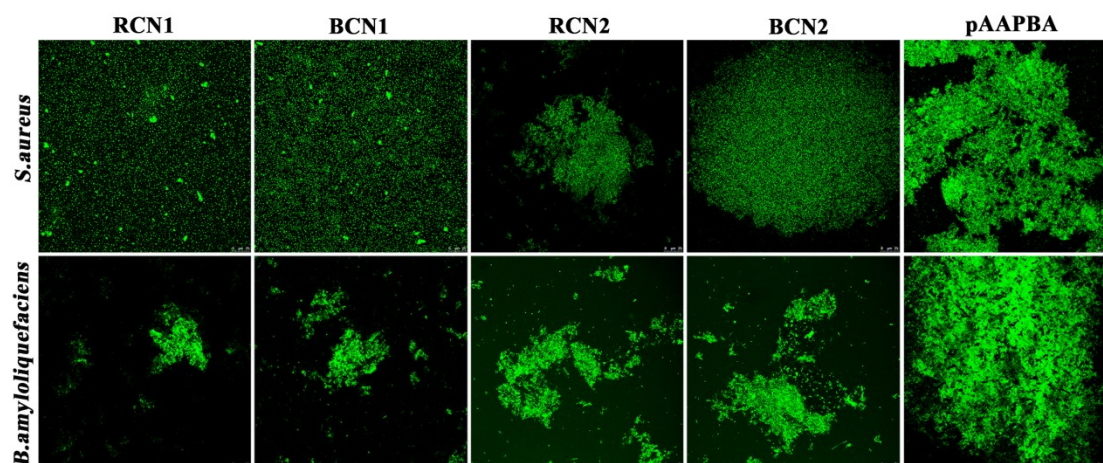


**Fig. S4** The adhesion activity to *S. aureus* and *B. amyloliquefaciens* observed by CLSM after treated with RCN1, BCN1, RCN2, BCN2 and pAAPBA60 for 2 h at 37°C, respectively.

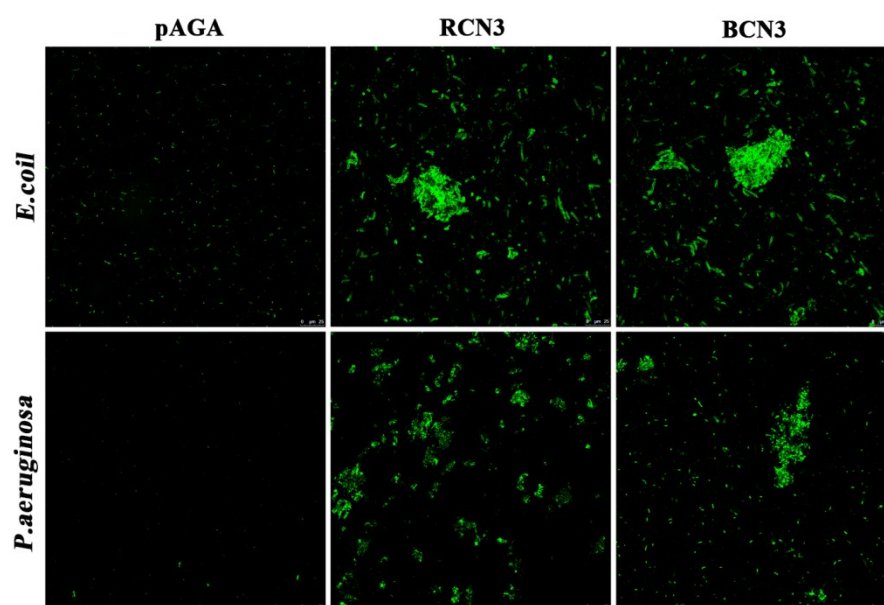


**Fig. S5** The adhesion activity to *E. coli* and *P. aeruginosa* observed by CLSM after treated with RCN3 and BCN3 for 2 h at 37°C, respectively.



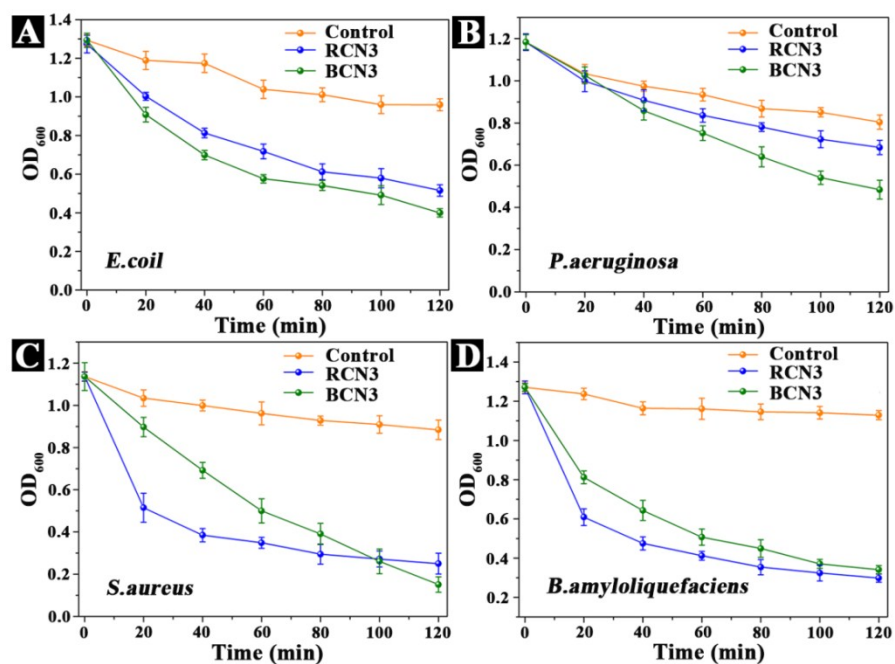


**Fig. S6** Agglutination of (A) *E. coli*; (B) *P. aeruginosa*, (C) *S. aureus* and (D) *B. amyloliquefaciens* after treated with RCN3 and BCN3.

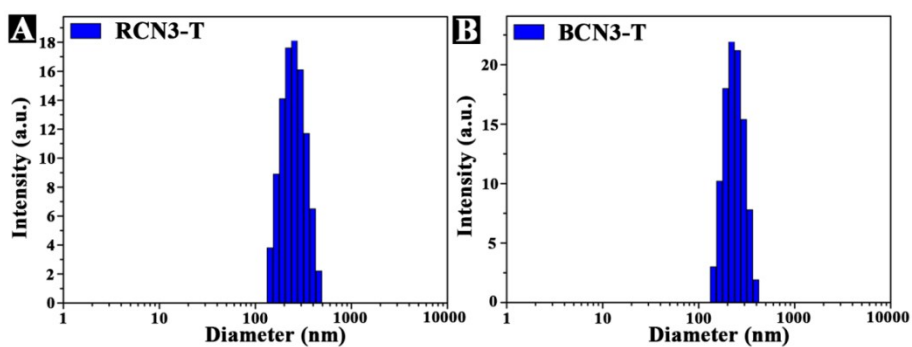


**Fig. S7** Size distribution of (A) RCN3-T and (B) BCN3-T in pH 7.4 PBS.

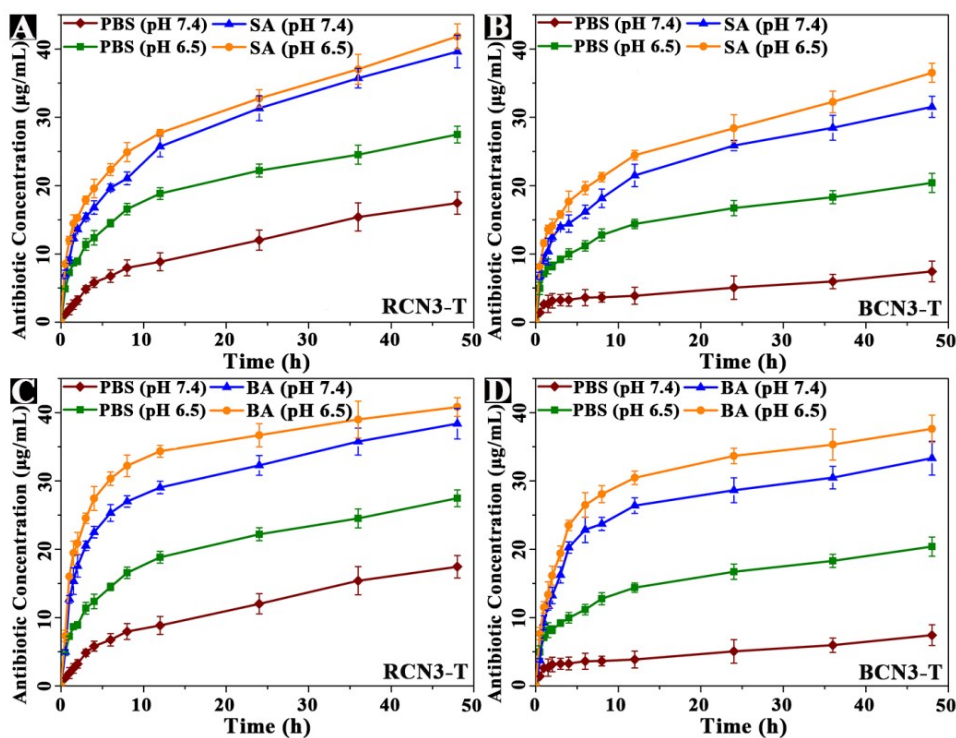


**Fig. S8** In vitro cumulative release of Triclosan from (A, C) RCN3-T and (B, D) BCN3-T in PBS buffer at pH 7.4 and 6.5 with or without the presence of (A, B) *S. aureus* and (C, D) *B. amyloliquefaciens*.

### Acid-Sensitivity of Copolymeric Nanoparticles.

It was reported that the formation of boronate esters between PBA and diols will perform under specific alkaline conditions (usually close to or higher than the  $pK_a$  of PBA) and the equilibrium of boric acid and its derivatives in the system will shift with the change of pH value.<sup>6-9</sup> The equilibrium diagram of boric acid with boronate was shown in [Scheme S1](#). When the pH value decreases, it is obviously that the boronate will be dissociated. It has been verified that the unique weak acid sensitive of boronate linkage imparted dynamic reversibility to the self-assembled nanoparticles.<sup>10</sup> Since the bacteria-induced infection site is normally slightly acidic (pH 6.0~6.6),<sup>11,12</sup> it is necessary to study the morphology variation of the copolymeric nanoparticles and their adhesion effectiveness to bacteria in the weak acid environment. As shown in [Table S3](#), the size of RCN3 increased from 149.6 nm at pH 7.4 to 176.1 nm at pH 6.5

while the size of BCN3 changed from 170.8 to 202.3 nm, demonstrating that the nanoparticle structure swelled when the pH value decreased from 7.4 to 6.5, indicating that the boronate tends to dissociate in weak acid conditions. Additionally, The zeta potential of BCN3 increased from -8.58 mV at pH 7.4 to -6.77 mV at pH 6.5 while the corresponding value of RCN3 decreased from -38.8 to -33.2 mV, resulting in the movement of dissociation equilibrium of boric acid derivatives followed by the decrease of the proportion of dissociated molecules.

The dissociation of boronate linkage was triggered by weak acidity (pH 6.5), which can be potentially applied for acid-responsive drug release system in the weak acid microenvironment at the infected site. To investigate whether the adhesion and aggregation behavior of copolymeric nanoparticles to bacteria will change at pH 6.5, the repetitive adhesion experiments of RCN3 and BCN3 to *S. aureus* and *B. amyloliquefaciens* were performed at pH 6.5 and images taken by CLSM are shown in Fig. S9. It can be seen that the adhesion effectiveness of two kinds of nanoparticles to *S. aureus* and *B. amyloliquefaciens* was not weakened obviously, and still had good adhesion capability in the weak acid environment.

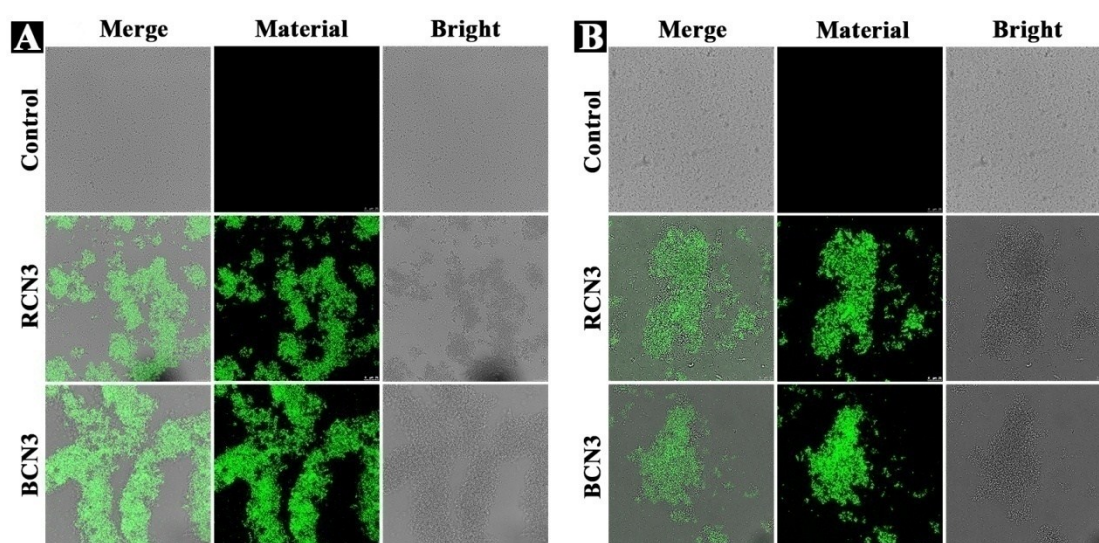


**Fig. S9** The adhesion capability to bacteria observed by CLSM of (A) *S. aureus*, (B) *B. amyloliquefaciens* after treated with PBS, RCN3 and BCN3 for 2 h at 37 °C (pH =

6.5), respectively. The concentration of all the copolymeric nanoparticles was 1 mg/mL. Green fluorescence: BODIPY molecule in fluorescence-labeling nanoparticles.

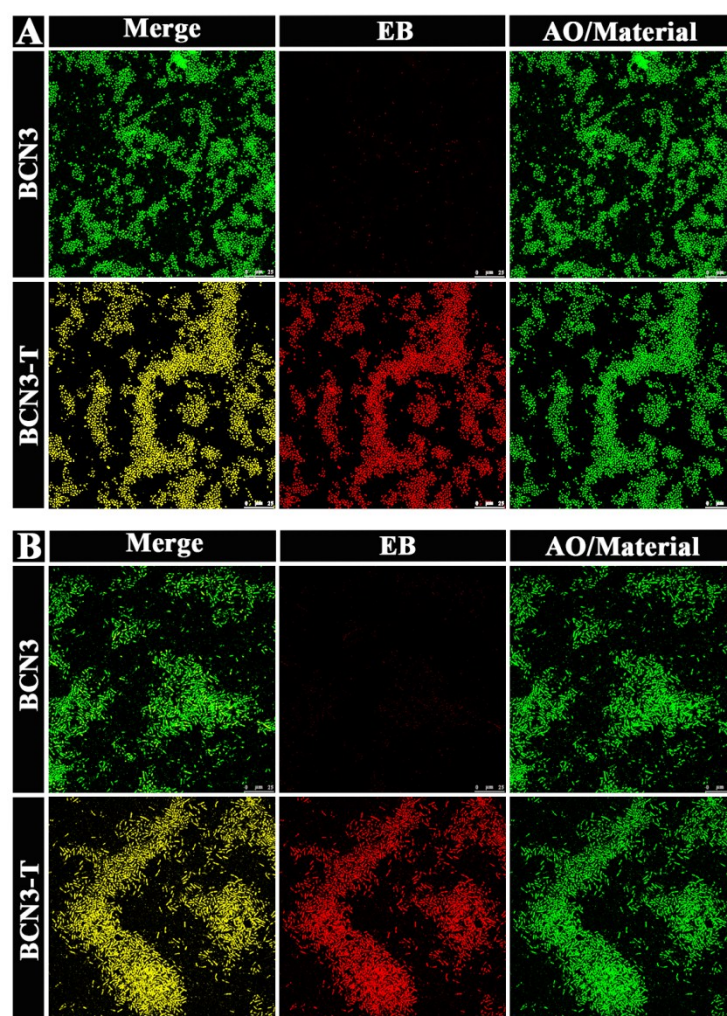


**Fig. S10** Antibacterial activity observed by CLSM of (A) *S. aureus*, (B) *B. amyloliquefaciens* after treated with PBS, BCN3 and BCN3-T, respectively



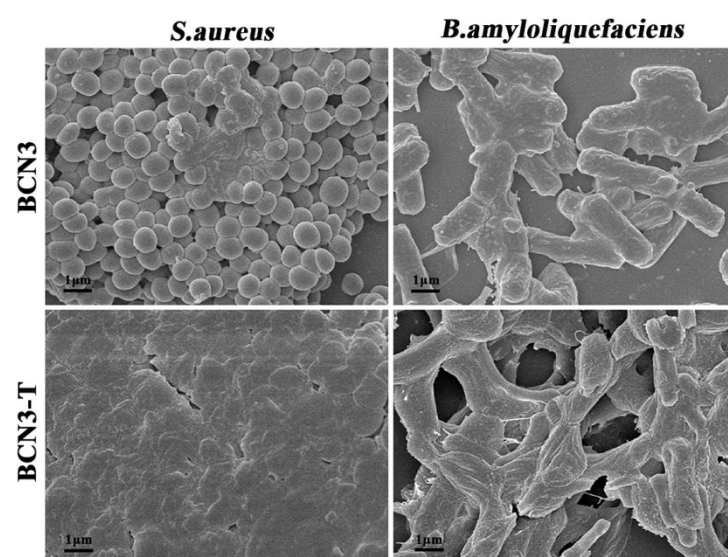


**Fig. S11** SEM images of *S. aureus* and *B. amyloliquefaciens* after treated with BCN3 and BCN3-T, respectively

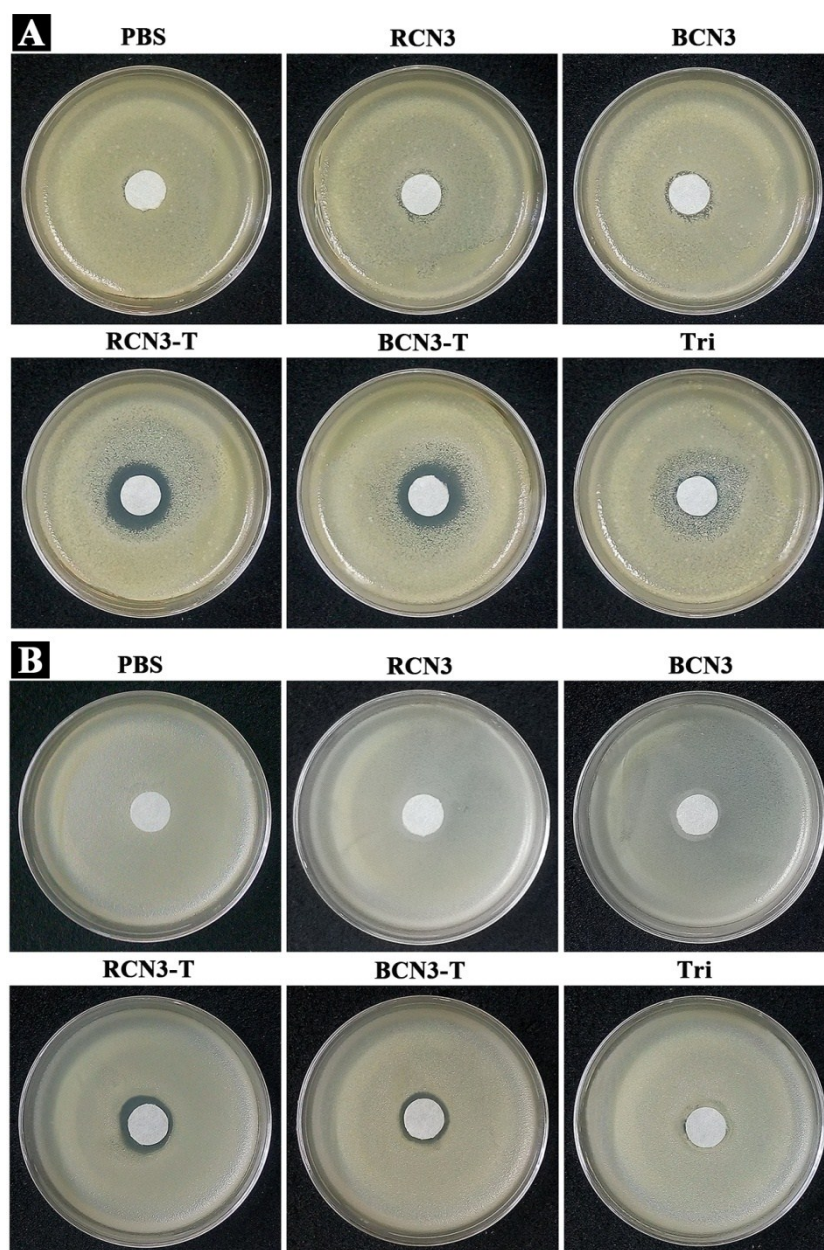


**Fig. S12** Inhibition zones of RCN3, BCN3, RCN3-T, BCN3-T as well as pure Triclosan solution against (A) *S. aureus* and (B) *B. amyloliquefaciens*. The concentration of Triclosan loaded in RCN3-T and BCN3-T was the same as that of free Triclosan solution.

**Table S1. Constitution of Amphiphilic Copolymers**

Sample	Monomer	RAFT agent	Conv (wt%) <sup>a</sup>	AAPBA/AGA (mol/mol)	
				Theory	<sup>1</sup> HNMR <sup>b</sup>
p(AAPBA <sub>15</sub> - <i>b</i> -AGA <sub>45</sub> )	AGA	pAAPBA <sub>15</sub>	86.64	0.33	0.27
p(AAPBA <sub>30</sub> - <i>b</i> -AGA <sub>30</sub> )	AGA	pAAPBA <sub>30</sub>	79.39	1.00	0.91
p(AAPBA <sub>45</sub> - <i>b</i> -AGA <sub>15</sub> )	AGA	pAAPBA <sub>45</sub>	75.41	3.00	3.24
p(AAPBA <sub>15</sub> - <i>r</i> -AGA <sub>45</sub> )	AGA/AAPBA	BODIPY-RAFT	88.70	0.33	0.32
p(AAPBA <sub>30</sub> - <i>r</i> -AGA <sub>30</sub> )	AGA/AAPBA	BODIPY-RAFT	78.02	1.00	1.00
p(AAPBA <sub>45</sub> - <i>r</i> -AGA <sub>15</sub> )	AGA/AAPBA	BODIPY-RAFT	77.76	3.00	3.16
pAAPBA <sub>60</sub>	AAPBA	BODIPY-RAFT	67.52	----	----
pAGA <sub>60</sub>	AGA	BODIPY-RAFT	92.01	----	----

<sup>a</sup> Calculated via weight method; <sup>b</sup> Calculated by means of the integral intensity of the <sup>1</sup>H NMR spectra.

**Table S2.** D<sub>H</sub>, PDI and Zeta potential of copolymeric nanoparticles (pH 7.4) measured by DLS at 25°C.

Sample <sup>a</sup>	D <sub>H</sub> (nm)	PDI	Zeta potential (mV)
RCN1	156.8 ± 3.8	0.14 ± 0.02	-17.0 ± 2.81
BCN1	141.7 ± 0.9	0.10 ± 0.05	-3.43 ± 0.23
RCN2	180.6 ± 5.4	0.12 ± 0.02	-25.3 ± 0.81
BCN2	188.3 ± 3.3	0.08 ± 0.03	-5.33 ± 0.20
RCN3	149.6 ± 0.3	0.05 ± 0.00	-38.8 ± 2.10
BCN3	170.8 ± 1.5	0.08 ± 0.03	-8.58 ± 0.32

<sup>a</sup> Nanoparticles of p(AAPBA<sub>15</sub>-*r*-AGA<sub>45</sub>), p(AAPBA<sub>30</sub>-*r*-AGA<sub>30</sub>), p(AAPBA<sub>45</sub>-*r*-AGA<sub>15</sub>) and p(AAPBA<sub>15</sub>-*b*-AGA<sub>45</sub>), p(AAPBA<sub>30</sub>-*b*-AGA<sub>30</sub>), p(AAPBA<sub>45</sub>-*b*-AGA<sub>15</sub>) were tabbed as RCN1, RCN2, RCN3 and BCN1, BCN2, BCN3, respectively.

**Table S3.** D<sub>H</sub>, PDI and zeta potential of copolymeric nanoparticles (pH 6.5) measured by DLS at 25°C.

	Sample	D <sub>H</sub> (nm)	PDI	Zeta potential (mV)
pH 7.4	RCN3	149.6 ± 0.3	0.05 ± 0.00	-38.8 ± 2.10
	BCN3	170.8 ± 1.5	0.08 ± 0.03	-8.58 ± 0.32
pH 6.5	RCN3	176.1 ± 0.7	0.10 ± 0.04	-33.2 ± 2.01
	BCN3	202.3 ± 1.9	0.14 ± 0.04	-6.77 ± 0.40

**Table S4.** Size, PDI, encapsulation efficiency (EE) and loading capacity (LC) of Triclosan-loaded copolymeric nanoparticles.

Sample	$D_H$ (nm)	PDI	EE (%)	LC (%)
RCN3-T	$229.4 \pm 4.6$	$0.14 \pm 0.01$	$76.7 \pm 1.3$	$18.7 \pm 1.5$
BCN3-T	$264.6 \pm 4.7$	$0.15 \pm 0.03$	$83.3 \pm 0.9$	$20.0 \pm 1.2$



## References

- 1 J. An, Q. Guo, P. Zhang, A. Sinclair, Y. Zhao, X. Zhang, K. Wu, F. Sun, H. C. Hung, C. Li and S. Jiang, *Nanoscale*, 2016, **8**, 9318-9327.
- 2 M.-C. Lee, S. Kabilan, A. Hussain, X. Yang, J. Blyth and C. R. Lowe, *Anal. Chem.*, 2004, **76**, 5748-5755.
- 3 S. R. S. Ting, E. H. Min, P. B. Zetterlund and M. H. Stenzel, *Macromolecules*, 2010, **43**, 5211-5221.
- 4 S. Peroche, G. Degobert, J. L. Putaux, M. G. Blanchin, H. Fessi and H. Parrot-Lopez, *Eur. J. Pharm. Biopharm.*, 2005, **60**, 123-131.
- 5 X. Jin, X. Zhang, Z. Wu, D. Teng, X. Zhang, Y. Wang, Z. Wang and C. Li, *Biomacromolecules*, 2009, **10**, 1337-1345.
- 6 J. Kim, Y. M. Lee, H. Kim, D. Park, J. Kim and W. J. Kim, *Biomaterials*, 2016, **75**, 102-111.
- 7 Y. Li, W. Xiao, K. Xiao, L. Berti, J. Luo, H. P. Tseng, G. Fung and K. S. Lam, *Angew. Chem., Int. Ed.*, 2012, **51**, 2864-2869.
- 8 G. Springsteen and B. Wang, *Curr. Opin. Microbiol.*, 2002, **58**, 5291-5300.
- 9 H. Liu, Y. Li, K. Sun, J. Fan, P. Zhang, J. Meng, S. Wang and L. Jiang, *J. Am. Chem. Soc.*, 2013, **135**, 7603-7609.
- 10 H.-Z. Jia, J.-Y. Zhu, X.-L. Wang, H. Cheng, G. Chen, Y.-F. Zhao, X. Zeng, J. Feng, X.-Z. Zhang and R.-X. Zhuo, *Biomaterials*, 2014, **35**, 5240-5249.
- 11 R. C. Mercier, *J. Antimicrob. Chemoth.*, 2002, **50**, 19-24.
- 12 C.-W. Hsiao, H.-L. Chen, Z.-X. Liao, R. Sureshbabu, H.-C. Hsiao, S.-J. Lin, Y. Chang and H.-W. Sung, *Adv. Funct. Mater.*, 2015, **25**, 721-728.